

## Scaling Law for the Partitioning of Energy in Fragmenting Multicharged Carbon Clusters

M. Chabot,<sup>1</sup> F. Mezdari,<sup>2,\*</sup> K. Béroff,<sup>2</sup> G. Martinet,<sup>1</sup> and P.-A. Hervieux<sup>3</sup>

<sup>1</sup>*Institut de Physique Nucléaire, IN2P3-CNRS and Université Paris-Sud, 91406 Orsay Cedex, France*

<sup>2</sup>*Laboratoire des Collisions Atomiques et Moléculaires, CNRS and Université Paris-Sud, 91405 Orsay Cedex, France*

<sup>3</sup>*Institut de Physique et Chimie des Matériaux de Strasbourg, CNRS and Université de Strasbourg BP 43, F-67034 Strasbourg, France*

(Received 23 July 2009; published 27 January 2010)

The complete fragmentation of highly excited and multicharged  $C_n^{q+}$  clusters ( $n = 5-10$ ;  $q = 2-4$ ), produced in high velocity collisions of  $C_n^+$  with atoms, has been measured. Multiplicity distributions are presented and used to deduce, within a statistical framework, the partitioning of energy between the fragments' production and fragments' kinetic energy. This partitioning is found to scale as the charge over mass ratio of the cluster.

DOI: 10.1103/PhysRevLett.104.043401

PACS numbers: 36.40.Qv

The fragmentation of molecules in high charge states has been studied in the last decades with high velocity collisions, electron impact, highly-charged ion low velocity collisions, intense and short lasers [1]. For high enough charges, when Coulomb forces exceed significantly the cohesive energy of the molecule, the latter vaporizes and the Coulomb repulsive energy is released into atomic fragments kinetic translational energy (KTER). This situation, referred to as Coulomb explosion, has been widely studied for small molecules such as diatomics and triatomics. In particular, a large amount of work has been devoted to a comparison between measured KTER and predictions of a simple point charge Coulomb model (PCCM). For particle induced ionization, measured KTER distributions were found in good agreement with PCCM predictions for average values, but considerably larger distributions were experimentally obtained. This was explained by the population, in the collision, of a variety of electronically excited states of more or less Coulombic character [2].

Much less is known on large molecules and clusters. Studies of the stability (appearance sizes) of multicharged species have been carried out as a function of the charge, size, internal energy for a variety of systems [3], but only partial information has been extracted concerning the fragmentation of these systems. This is due to the fact that only a small part of all emitted fragments are detected in experiments, neutral fragments being usually missing. From a theoretical point of view, the role of the fissibility parameter on the stability and on the fragmentation pattern of highly-charged clusters has been put forward [4]. But in none of these studies was the relaxation of highly excited multicharged clusters considered. Indeed, depending on from which shells the electrons are removed, low excited or highly excited multicharged systems are produced.

When atomization from Coulomb interaction is not achieved, the internal energy may relax along two ways: the production of a variable number of fragments (atoms and/or molecules) and kinetic energy release (KER), including fragments translational energy but also vibrational and rotational energy for the case of molecular fragments.

How this sharing is operating, depending on the cluster charge, size and internal energy, is an open question that we address in this Letter. The interest for this question goes beyond the case of atomic clusters. Indeed, the role of Coulomb interaction in the fragmentation of highly excited unstable nuclei is actively studied [5] and its understanding is important in other fields such as the comprehension of supernova dynamics or neutron star properties [6].

For this study, we performed measurements of fragmentation branching ratios of multicharged and highly excited carbon clusters created in high velocity collisions. A large and quite unexplored domain of Coulomb energy over cohesive energy ratios [0.05–1] has been investigated by ranging the cluster size from  $n = 5$  to  $n = 10$  and the cluster charge from  $q = 2$  to  $q = 4$ . The internal energy of the clusters was extracted on the basis of experimental results and calculations as will be seen below. The link between internal energy and measured fragmentation branching ratios, analyzed within a statistical context, provided the partitioning of energy in these systems. The experiment was performed at the Tandem accelerator in Orsay. Beams of incident  $C_n^+$  clusters ( $n = 5-10$ ) were produced at  $2n$  MeV energy and collided with a helium atom. Following single and multiple ionization, electronically excited multicharged clusters  $C_n^{q+}$  ( $q \geq 2$ ) were produced. All details about the apparatus and the way fragmentation is fully measured within a [0–100] ns time window have already been published [7,8]. The set of data is a huge one, for example, 85 different channels were observed in the fragmentation of  $C_{10}^{4+}$  [9]. Only the multiplicity (number of final fragments) distributions will be used in the present analysis. Such experimental multiplicity distributions are presented in Fig. 1 for  $C_n^{q+}$  with  $n = 5, 7, 10$  and  $q = 2-4$ .

In a microcanonical statistical framework, fragmentation of clusters depends only on their internal energy and the link between the two is expressed as:

$$p(m) = \int_0^\infty f(E^*)p(m, E^*)dE^*, \quad (1)$$

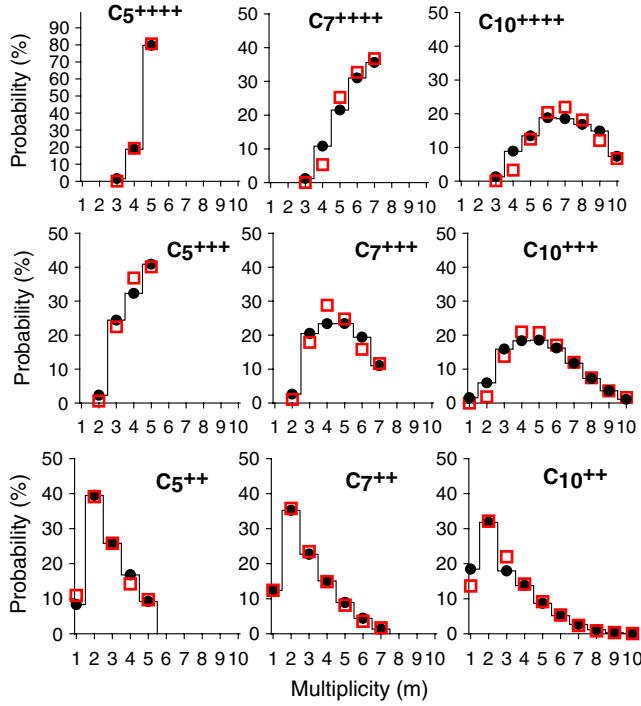


FIG. 1 (color online). Experimental (filled circles) and fitted (open squares) multiplicity distributions of  $C_n^{q+}$  clusters with  $n = 5, 7, 10$  and  $q = 2-4$ .

where  $m$  is the multiplicity,  $p(m)$  is the multiplicity probability,  $p(m, E^*)$  the same quantity but at fixed cluster internal energy  $E^*$ , and  $f(E^*)$  is the normalized cluster internal energy distribution. We made our analysis of the fragmentation in this context, despite the fast fragmentation expected in these multicharged species ( $\sim$  ps). The reason is that statistics over a large amount of events ( $\sim 10^5$ ) is performed in our experiments, each collision being different from the preceding one according to the properties of the incident  $C_n^+$  cluster (temperature, isomer, orientation, collision impact parameter) and ionization process (electronic configuration). Then, a large volume of states is associated to a given final cluster internal energy. Based on the microcanonical Metropolis Monte Carlo (MMMC) statistical treatment of the fragmentation of neutral [7,10] and singly charged [9] carbon clusters, rectangle functions of adjustable widths  $\alpha$  and  $\beta$  were used for  $p(m, E^*)$  (see Fig. 2). The minimum multiplicity  $m_{\min}$  depends on the cluster charge (see Fig. 1). It is equal to 1 for  $q = 0-2$  but, since these species are unstable [11,12], equal to 2 and 3 for  $q = 3$  and  $q = 4$ , respectively [13]. The  $\alpha$  parameter represents the minimum energy where extra fragmentation above the minimum multiplicity starts; when  $m_{\min} = 1$ ,  $\alpha$  is the lowest dissociation energy. The  $\beta$  parameter represents the energetic cost of each extra fragment (supposed to be in its electronic ground state); it includes dissociation energy ( $E_{\text{diss}}$ ) and average KER. In neutral [7,10] and singly charged [9] carbon clusters,  $\alpha$  and  $\beta$  are weakly dependent on the cluster size and  $\alpha \sim 6$  eV,  $\beta \sim 7$  eV on average.

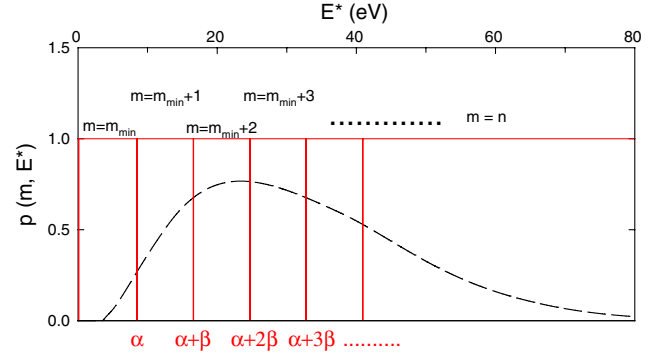


FIG. 2 (color online). Solid lines: Generic  $p(m, E^*)$  curves used in Eq. (1);  $m_{\min}$  is the minimum multiplicity of the cluster (see text), and  $\alpha$  and  $\beta$  adjustable parameters. Broken curve: One example of  $f(E^*)$  distribution used in Eq. (1), case of  $C_n^{q+}$ , with  $n = 10$  and  $q = 3$ .

The internal energy of a  $C_n^{q+}$  cluster is defined as the energy above the ground state of  $C_n^{q+}$ . For  $q = 2$  and  $n \geq 5$ , all  $C_n^{q+}$  clusters are predicted to be stable in their ground states [11]; internal energies are referenced with respect to the ground states of these intact species. For  $q = 3, 4$ , all species are predicted to be unstable [13]; internal energies have been referenced with respect to dissociated species. This internal energy has many origins in our experimental situation: the internal energy of incident hot  $C_n^+$  clusters ( $E_{\text{inc}}$ ), the internal energy associated to ionization of inner-valence electrons giving rise to electronically excited multicharged species ( $E_{\text{ion}}$ ), and for unstable species ( $q = 3, 4$ ) the potential Coulomb energy  $E_{\text{coul}}$ . Energy distributions of incident  $C_n^+$ ,  $f(E_{\text{inc}})$ , depend on  $n$  and have been presented elsewhere [14]; average values range from 3.5 eV for  $n = 5$  to 5.5 eV for  $n = 10$ . Energy distributions from Coulomb repulsion  $f(E_{\text{coul}})$  were calculated within the PCCM. Ionized atomic sites were obtained with the independent atom and electron collision model [8] using  $C_n^+$  equilibrium geometries. We present in Fig. 3 mean values and standard deviations for  $f(E_{\text{coul}})$  distributions. A strong  $n$  and  $q$  dependence is obtained for this Coulomb energy. Since the cohesive energy of clusters is approximately equal to  $6(n - 1)$  eV [15] we see that ratios of Coulomb energy over cohesive energy range roughly from 0.05 to 1 as mentioned before.

The energy distribution associated to Single Ionization  $f(E_{\text{ion}}^{\text{SI}})$  was extracted from experiment and checked by calculation. Indeed, for large size doubly charged clusters, the Coulomb contribution is small as compared to the neutral cluster cohesive energy, and we may expect  $\alpha$  and  $\beta$  values to be those of neutral and singly charged carbon clusters. Making this assumption for  $C_{10}^{q+}$  we have extracted, using Eq. (1) with  $p_{\text{exp}}(m)$  of Fig. 1,  $m_{\min} = 1$ ,  $\alpha = 6$  eV and  $\beta = 7$  eV, the total internal energy  $f(E^*)$  of  $C_{10}^{q+}$ . Then, after subtraction of  $f(E_{\text{inc}})$  from  $f(E^*)$  [see Eq. (2)], we obtained an experimental determination of  $f(E_{\text{ion}}^{\text{SI}})$ . This distribution is reported in Fig. 4. Note that a

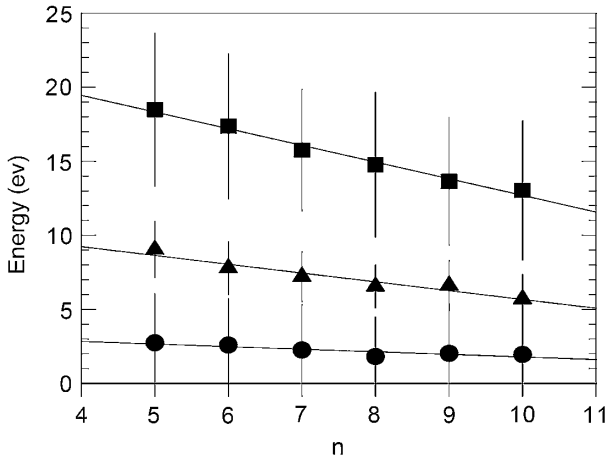


FIG. 3. Average values (symbols) and standard deviations (vertical lines) of the calculated Coulomb energy distributions  $f(E_{\text{coul}})$  in  $C_n^{q+}$ . Circles,  $q = 2$ ; triangles,  $q = 3$ ; squares,  $q = 4$ .

close distribution was obtained when following the same procedure but starting with  $C_9^{++}$  instead of  $C_{10}^{++}$ . On the other hand, calculations were performed, as explained elsewhere [16], using theoretical electron binding energies, pole strengths in  $C_n$  clusters, and the independent atom and electron collision model. Calculated distributions were found very weakly dependent on  $n$ ; the case of  $n = 10$  is presented in Fig. 4. The agreement between experiment and calculation is rather good, especially when considering the fact that calculations in the high energy domain are expected to be less accurate [17]. In the analysis, we used the experimental distribution of Fig. 4 for all  $n$  values.

For energy distributions associated to double  $f(E_{\text{ion}}^{\text{DI}})$  and triple  $f(E_{\text{ion}}^{\text{TI}})$  ionization, we assumed independent energy deposits of each ionization. This approximation relies on the independent electron approximation and is valid if relative molecular energies are not changing much with the charge. Finally, we may write:

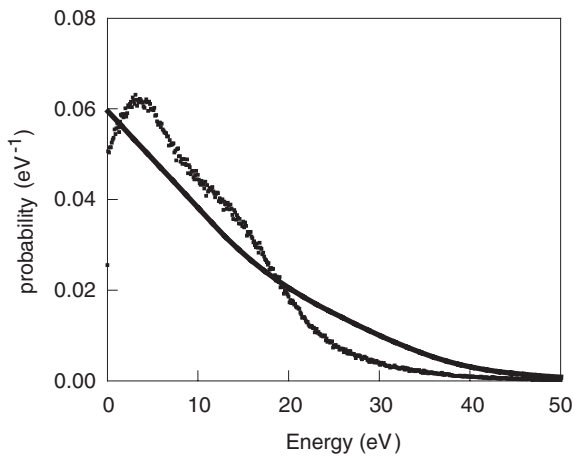


FIG. 4. Experimental (solid line) and calculated (symbols) internal energy distributions due to single ionization  $f(E_{\text{ion}}^{\text{SI}})$ .

$$\begin{aligned}
 f(E^*(n, q = 2)) &= f(E_{\text{inc}}(n)) \otimes f(E_{\text{ion}}^{\text{SI}}) \\
 f(E^*(n, q = 3)) &= f(E_{\text{inc}}(n)) \otimes f(E_{\text{ion}}^{\text{SI}}) \otimes f(E_{\text{ion}}^{\text{SI}}) \\
 &\quad \otimes f(E_{\text{coul}}(n, q = 3)) \\
 f(E^*(n, q = 4)) &= f(E_{\text{inc}}(n)) \otimes f(E_{\text{ion}}^{\text{SI}}) \otimes f(E_{\text{ion}}^{\text{SI}}) \otimes f(E_{\text{ion}}^{\text{SI}}) \\
 &\quad \otimes f(E_{\text{coul}}(n, q = 4)), \quad (2)
 \end{aligned}$$

where the symbol  $\otimes$  means convolution of energy distributions. Using Eq. (2) we found internal energy distributions having average values around 15 eV, 30 eV, 50 eV, respectively, for doubly, triply, and quadruply charged clusters. In all cases, the main contribution is coming from the excitation term  $E_{\text{ion}}$ . On the basis of these known  $f(E^*)$  and using experimental multiplicity distributions  $p(m)$ , we searched, for each  $C_n^{q+}$  cluster, the  $p(m, E^*)$  function able to fulfill Eq. (1). Results of the  $\alpha$  and  $\beta$  parameters leading to the best fits are presented in Table I. Error bars in the order of 15% and 8% for  $\alpha$  and  $\beta$ , respectively, were obtained by using slightly different  $f(E_{\text{ion}}^{\text{SI}})$  distributions. Results of the fits are reported in Fig. 1 for  $n = 5, 7, 10$  and  $q = 2-4$ . A very good adjustment between experiment and calculation was also obtained for  $n = 6, 8, 9$  and  $q = 2-4$  (not shown). As seen from Table I,  $\beta$  values are always above 7 eV, especially for small and highly-charged clusters. This shows that a larger kinetic energy is imparted to neutral and singly charged fragments coming from the dissociation of multi-charged parents, as compared to neutral and singly charged fragments coming from the dissociation of neutral and singly charged parents.

In order to quantify this effect, we introduced the quantity  $p_k = (\beta - E_{\text{diss}})/\beta$  which represents the part of the internal energy dissipated into the fragments' kinetic energy. We calculated  $p_k$  values using  $\beta$  values from Table I and using  $E_{\text{diss}} = 6$  eV which is the mean dissociation energy in neutral and singly charged extra fragments [11]. Values of  $p_k$  are reported, as a function of the  $q/n$  ratio, in Fig. 5. Remarkably, we observe that all results align on a unique curve. This indicates that the cluster internal energy, and, in particular, its dominant contribution  $E_{\text{ion}}$ , dissipates more and more into the fragment's KER as  $q/n$  increases.

TABLE I. Values of  $\alpha$  and  $\beta$  parameters leading to the best fits of experimental multiplicity distributions of Fig. 1.

$n$	$q = 2$		$q = 3$		$q = 4$	
	$\beta$ (eV)	$\alpha$ (eV)	$\beta$ (eV)	$\alpha$ (eV)	$\beta$ (eV)	$\alpha$ (eV)
5	9.7	4.0	13.0	8.5	17.7	17.5
6	9.1	5.0	10.9	10.0	16.3	15.0
7	8.2	5.0	10.7	7.5	13.7	13.5
8	7.7	5.0	9.5	9.0	12.5	11.5
9	7.5	6.0	9.1	8.5	10.6	13.5
10	7.0	6.0	8.1	8.5	9.1	12.5

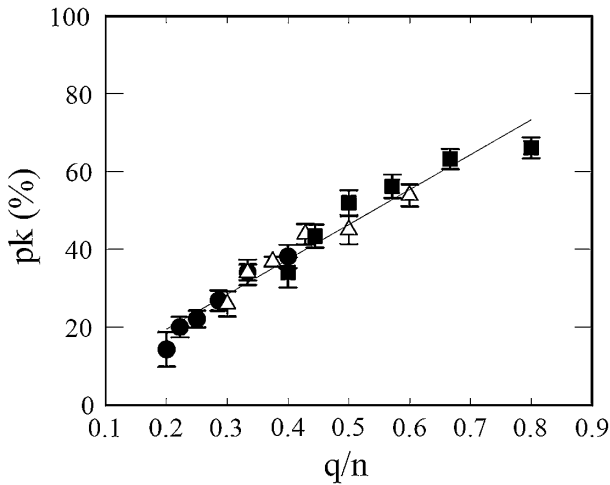


FIG. 5. Part of the internal energy dissipated in KER, in percent, as a function of the cluster charge over mass ratio  $q/n$ ; circles  $q = 2$ , triangles  $q = 3$ , squares  $q = 4$ ; the solid line is a linear regression of the data.

According to previous works performed on diatomics [18], steeper and steeper potential energy curves of electronic excited states and an increase of the number of repulsive states should occur when increasing the charge. It will have the effect of converting more and more into KTER, the internal energy of the cluster. On the other hand, the steepness of the potential energy curves is related to the number of electrons available to screen the charges. At fixed  $q$ , the steepness should then decrease with the size. We believe these two trends explain, qualitatively, the result of Fig. 5. Note that these trends are expected in all multicharged systems. In a quantitative way, it is interesting to test whether the  $p_k$  observable is connected in some way to the fissibility parameter  $X$  of the cluster, which is a measure of the relative Coulomb interaction. This is defined, in the liquid drop model [3], as  $E_{\text{coul}}/(2 * E_{\text{surf}})$  where  $E_{\text{surf}}$  is the surface part of the cohesive energy. For linear multicharged small carbon clusters [11,12], this surface part is not defined, and we introduced the fissibility parameter of the chain  $X_{\text{chain}}$  as the ratio of the Coulomb energy over twice the cohesive energy. According to a classical electrostatic model, the Coulombic energy of a small chain of length  $L$  and radius  $r$  ( $r \ll L$ ) carrying a uniform charge  $q$  is  $E_{\text{coul}} = (q^2/4\pi\epsilon_0 L) * \ln(L/r)$  [19]. On the other hand, the cohesive energy is, as seen before, proportional to  $(n - 1)$ . As  $L = (n - 1) * a$ , where  $a$  is the interatomic distance, and since the logarithm term is slowly varying with  $L$ , we see that  $X_{\text{chain}}$  is found proportional to  $q^2/(n - 1)^2$ . This result is in quantitative disagreement with the scaling law obtained for  $p_k$ . It shows that the interpretation of this scaling law deserves a much deeper theoretical investigation.

To summarize, we presented in this Letter experimental results concerning the fragmentation of multicharged and highly excited carbon clusters produced in high velocity

collisions between  $C_n^+$  beams ( $n = 5-10$ ) and the atomic He target. Thanks to the detection of all fragments, experimental multiplicity distributions were obtained for  $C_n^{q+}$  clusters  $n = 5-10$ ,  $q = 2-4$  and analyzed within a statistical context, using Eq. (1). In the latter, semiempirical internal energy distributions  $f(E^*)$  were introduced and two parameters  $\alpha$  and  $\beta$ , parameterizing  $p(m, E^*)$  functions, adjusted in order to fit calculated multiplicity distributions to experimental ones. From the obtained  $\beta$  values, the part of the internal energy of  $C_n^{q+}$  clusters used in fragments kinetic energy was extracted. This part was found to scale as the charge over mass ratio. This result illustrates for the first time, through qualitative and quantitative aspects, the role of the Coulomb perturbation in the partitioning of energy of fragmenting multicharged clusters. The investigated domain is rather broad (ratio of Coulomb energy over cohesive energy varying between 0.05 and 1) and the result believed to be of general application, i.e., not dependent on the cluster type.

The authors thank P. Désesquelles, L. Lavergne, and A. LePadellec for their help during the experiments.

\*Present address: University of Gabès (Tunisia)

- [1] D. Mathur, Phys. Rep. **391**, 1 (2004).
- [2] M. Tarisien *et al.*, J. Phys. B **33**, L11 (2000); B. Siegmann *et al.*, Phys. Rev. A **62**, 022718 (2000).
- [3] U. Naher *et al.*, Phys. Rep. **285**, 245 (1997); B. Manil *et al.*, Phys. Rev. Lett. **91**, 215504 (2003); S. Diaz-Tendero, M. Alcami, and F. Martin, Phys. Rev. Lett. **95**, 013401 (2005).
- [4] I. Last, Y. Levy, and J. Jortner, J. Chem. Phys. **123**, 154301 (2005); F. Calvo, Phys. Rev. A **74**, 043202 (2006).
- [5] V. Baran *et al.*, Nucl. Phys. A **703**, 603 (2002).
- [6] G. Lehaut, F. Gulminelli, and O. Lopez, Phys. Rev. Lett. **102**, 142503 (2009).
- [7] G. Martinet *et al.*, Phys. Rev. Lett. **93**, 063401 (2004).
- [8] F. Mezdari *et al.*, Phys. Rev. A **72**, 032707 (2005).
- [9] F. Mezdari, Ph.D. thesis, University Paris 6, 2005 (unpublished).
- [10] S. Diaz-Tendero *et al.*, Int. J. Mass Spectrom. **252**, 126 (2006).
- [11] S. Diaz-Tendero *et al.*, Braz. J. Phys. **36**, 529 (2006).
- [12] G. Sanchez, Master thesis, Universidad Autonoma de Madrid, 2006 (unpublished).
- [13] With the exception of  $C_{10}^{+++}$  which is the lowest size  $C_n^{+++}$  cluster having a stable electronic ground-state [12].
- [14] M. Chabot *et al.*, J. Phys. B **39**, 2593 (2006).
- [15] L. Montagnon and F. Spiegelman, J. Chem. Phys. **127**, 084111 (2007), and references therein.
- [16] K. Béroff *et al.*, Nucl. Instrum. Methods Phys. Res., Sect. B **267**, 866 (2009).
- [17] M. S. Deleuze *et al.*, J. Chem. Phys. **111**, 5851 (1999).
- [18] P. J. Bruna and J. S. Wright, J. Phys. B **26**, 1819 (1993); J. S. Wright *et al.*, Phys. Rev. A **59**, 4512 (1999).
- [19] J. D. Jackson, *Classical Electrodynamics* (John Wiley and Sons, New York, 1975).